Thermotropic Biaxial Nematic Phase in Liquid Crystalline Organo-Siloxane Tetrapodes

K. Merkel,[1] A. Kocot,[1,2] J. K. Vij,[1,*] R. Korlacki,[1] G. H. Mehl,[3] and T. Meyer[3]
[1]*Trinity College, University of Dublin, Dublin 2, Ireland*
[2]*University of Silesia, Katowice, Poland*
[3]*University of Hull, Hull, United Kingdom*
(Received 25 July 2004; published 2 December 2004)

Infrared absorbance measurements have been carried out on two liquid crystalline organo-siloxane tetrapodes. Results unambiguously show the existence of a biaxial nematic phase below a uniaxial nematic phase. The three components of IR absorbance are used to calculate the various order parameters. On cooling, a weak first-order transition from isotropic to nematic is observed, followed by a second-order phase transition to biaxial nematic where the biaxiality parameters are found to be significantly large. Results are supported by observations from conoscopy and texture. Temperature dependences of the order parameters are well explained by the mean-field model for a biaxial phase.

DOI: 10.1103/PhysRevLett.93.237801 PACS numbers: 61.30.Gd, 61.30.Eb, 78.30.Jw

Through a generalization of the Meier-Saupe theory of the nematic phase in thermotropic liquid crystals, Freiser [1] predicted a biaxial nematic phase with two orthogonal optic axes. This phase was suggested to arise from a second-order transition from uniaxial to biaxial (N_U to N_B) at a temperature lower than the isotropic to uniaxial nematic (I-N_U) phase. The prediction led to a considerable flurry in both theoretical and experimental works. Yu and Saupe discovered in 1980 a biaxial nematic phase, in a lyotropic liquid crystal system, sandwiched in between a uniaxial positive and a uniaxial negative nematic phase [2]. Since this discovery, a number of works on biaxiality in nematics have appeared in the literature and this has attracted considerable interest; it continues to date to be a highly debated subject [3–11]. The earlier reports of the observation of biaxiality in nematics using optical techniques were not confirmed from the results obtained using NMR spectroscopy [12,13], widely believed to prove whether or not the biaxiality is present. The molecular shape is the governing factor for the observation of biaxiality. It was shown particularly in [7] that a ring shaped trimeric liquid crystal undergoes a uniaxial-to-biaxial nematic phase transition as a function of temperature, though the authors used only qualitative indicators. Recently, two Letters have reported the detection of a biaxial nematic phase in thermotropic liquid crystals composed of bow shaped molecules [14–16]. The biaxiality has also recently been confirmed in a side chain liquid crystalline polymer [17].

In this Letter, two liquid crystalline (LC) tetrapodes with two different mesogen systems [Figs. 1(a) and 1(b)] are shown to exhibit biaxiality in the nematic phase experimentally. Polarized IR spectroscopy is used in determining the biaxiality order parameters, and results on biaxiality are supported by conoscopy and texture. An essential aim of this effort has been the investigation of materials, which are chemically uniform thus avoiding problems associated with polydispersity and the coil structure of a linear polymer. For such supermolecular systems, the properties are found to be indeed different from those of low molar mass LCs and related polymers [18]. The tetrapodes exhibit biaxiality close to the ambient temperature; the temperature range of both uniaxial and biaxial phases is quite wide especially for one of the two tetrapodes studied. This also facilitates the ease by which a range of complimentary techniques can be used to explore the biaxiality. The observation of biaxial nematic is the first quantitative observation in a new class of liquid crystals. In the tetrapodes the mesogens are connected to the siloxane core through four siloxane spacers, and the system forms a quasiflat platelet [Fig. 1(c)]. In order to achieve the optimized packing of the constituents, the mesogens are tilted in the plane of the platelet. Such a local structure of the LC tetrapodes in the nematic phase has been confirmed by x-ray diffraction [19] and molecular dynamics in the PVT conditions [20]. The key aspect of this approach has been to produce a biaxial nematic by hindering the rotation of rodlike mesogens around their respective long axes by linking these laterally through flexible siloxane spacers to a fixed siloxane core [see Figs. 1(a)–1(c)].

Infrared experiments on two tetrapodes [Figs. 1(a) and 1(b)] are used to obtain the order parameters, and results are analyzed in terms of the mean-field model. In the

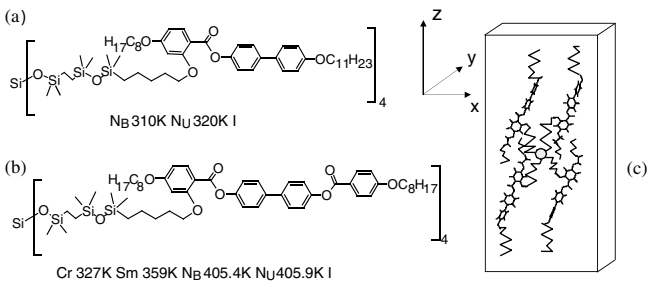

FIG. 1. Molecular structures of tetrapodes: (a) ***A*** and (b) ***B*** with asymmetric and symmetric mesogens, respectively. (c) Platelet formed by a macromolecule of the tetrapode ***A***.

model proposed by Straley [21] a general biaxial phase is described by the four scalar order parameters S, P, D, and C. Order parameters are defined as [22]

$$S \equiv S^Z_{zz}, \qquad D \equiv S^Z_{xx} - S^Z_{yy},$$
$$C \equiv (S^X_{xx} - S^X_{yy}) - (S^Y_{xx} - S^Y_{yy}), \quad \text{and} \quad P \equiv S^X_{zz} - S^Y_{zz}.$$

$S^i_{\alpha\beta}$ are the three diagonal Saupe ordering matrices, one for each of the three axes, $i = X, Y, Z$ (laboratory or phase axis); $\alpha = x, y, z$ (molecular axes); $S^i_{\alpha\beta} = \langle \frac{1}{2}(3l_{i,\alpha}l_{i,\beta} - \delta_{\alpha\beta})\rangle$. $l_{i,\alpha}$ and $l_{i,\beta}$ are the cosines of the angle between the molecular axis α and β with the laboratory axis i; z is fixed to the direction of the long molecular axis. The order parameter S^Z_{zz} is a measure of the average direction of molecular axis z with respect to the laboratory axis Z, whereas D is a measure of the molecular biaxiality for a uniaxial phase and is the difference between the distribution of x and y axes with respect to the Z axis. C is an intrinsic or molecular biaxiality parameter for a biaxial phase. P (the phase biaxiality of the system) is a measure of the difference in the probabilities of finding the z axis along the X and Y axes of the laboratory system. There are two ways for the system to become biaxial. The distribution function f is isotropic in φ (the azimuthal angle of the long molecular axis) but anisotropic in ψ (the rotation of the molecule around the molecular axis being biased, i.e., $D \neq 0$), which leads to $P = 0$, but $C \neq 0$, i.e., intrinsic biaxiality that corresponds to a natural tendency of the biaxial molecules to orient parallel to each other. On the other hand, a function f anisotropic in φ but isotropic in ψ gives $P \neq 0$, but $C = 0$. An extrinsic biaxiality, which under appropriate external causes can also be exhibited by cylindrically symmetric molecules, is represented by only two scalar order parameters, S and P.

The three spatial components of the IR absorbance have been measured for the planar homogenous and homeotropic sample geometries: one along and the two perpendicular to the nematic director. The homogenously oriented sample was obtained by coating ZnSe windows with nylon 6/6 solution in methanol. Homeotropic alignment was obtained by coating KBr windows by a carboxylatochromium complexes (chromolane) solution. Two monocrystalline KBr windows with their easy axes oriented parallel to each other were used as the IR cell. The short axes with intermediate n are aligned along this easy axis. The phenyl stretching band (1160 cm^{-1}) is found to be an excellent indicator of both the nematic and the biaxial ordering. The temperature range of the uniaxial and biaxial phases is established by direct observation of the absorbance components A_X and A_Y, as shown in Fig. 2 for tetrapode with asymmetric mesogen [Fig. 1(a), called ***A***]. Two regions in the nematic phase can easily be distinguished: one uniaxial where the two perpendicular absorbance components are equal and the second biaxial where A_X starts to exceed A_Y. This implies that the mesogens on the average are tilted along the X direction, resulting into the biaxial ordering of the tetrapode. Three components of absorbance are expressed in terms of these order parameters [22,23]:

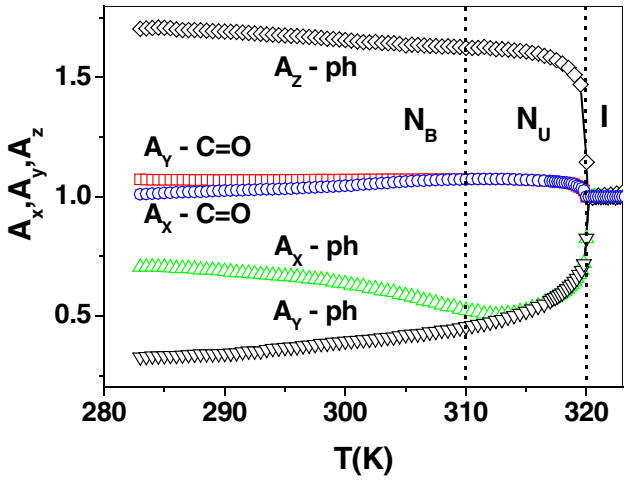

FIG. 2 (color online). Absorbance components normalized with those of the isotropic phase for ***A***: △, A_X; ▽, A_Y; ◇, A_Z values for its phenyl ring stretching band 1160 cm^{-1}; □, A_Y and ○, A_X values for the carbonyl stretching band 1738 cm^{-1} A_X and A_Y are measured for the homeotropically aligned sample.

$$A_X/A_0 = 1 + (S - P)(\tfrac{3}{2}\sin^2\beta - 1) + \tfrac{1}{2}(D - C) \times (\sin^2\beta\cos 2\phi), \quad (1)$$

$$A_Y/A_0 = 1 + (S + P)(\tfrac{3}{2}\sin^2\beta - 1) + \tfrac{1}{2}(D + C) \times (\sin^2\beta\cos 2\phi), \quad (2)$$

$$A_Z/A_0 = 1 + S(2 - 3\sin^2\beta) - D\sin^2\beta\cos 2\phi, \quad (3)$$

where β is the angle between the transition dipole moment and the z axis; ϕ is the azimuthal angle of the transition moment measured with respect to the x axis. In order to determine whether branches of the tetrapode are aligned homeotropically, i.e., normal to the substrate, the absorbance components for the two methylene stretching bands [symmetric (2900 cm^{-1}) and asymmetric (2800 cm^{-1})] are examined. The results give S ($\cong 0.3$), which is a typical value of S for an orthogonal alignment of the chain as in the Sm*A* phase, and negligible values for D, P, and C parameters. These results show that the alignment of the chain is indeed homeotropic. S and P for the mesogens are found by employing the phenyl stretching band (1160 cm^{-1}) for the homeotropic aligned sample in the equations [(1) and (2)]. First S and P are calculated for the mesogen using the vibrational frequency of the phenyl stretching band for which β is zero. P is also given as $P \cong \frac{4S-1}{2}\langle\sin^2\theta\rangle$ [23]; θ is the tilt angle of the mesogen. Since the transition moment of the phenyl stretching band is parallel to the mesogen, θ can now be considered to be the polar angle β of the phenyl stretching band in the platelet system of reference.

We thus obtain a set of four equations for A_X and A_Y for the two bands: phenyl (1160 cm^{-1}) and the carbonyl (1738 cm^{-1}) stretching, and hence four parameters for the platelet are calculated.

The observed sequence of the phase transitions (Fig. 3) is found to be the following: transition at a higher temperature leads to the uniaxial-isotropic phase transition where both S and D are different from zero; the second transition occurs at a lower temperature, where both P and C are also nonzero. Relatively large values of the biaxiality order parameters and their increase with decreasing temperature provide the first quantitative proof for the observation of biaxiality in the nematic phase of a tetrapode shown in Fig. 1(a). Since the absolute values of the order parameters have been determined, the mean-field model for a biaxial nematic phase can therefore be easily tested. Free energy as a function of the second δ and third Δ fundamental invariants of the order tensors of the system [24] is given as

$$F = \frac{a}{2}\delta + \frac{b}{3}\Delta + \frac{c}{4}\delta^2 + \frac{d}{5}\delta\Delta + \frac{e}{6}\Delta^2 + \frac{e'}{6}\delta^3 + \ldots, \quad (4)$$

where $\delta = (3S^2 + P^2)/2$ and $\Delta = 3S(S^2 - P^2)/4$. In the simplest form of the model, a is assumed to be a linear function of temperature, $a = \alpha(T - T^*)$, and b and the higher order coefficients are essentially independent of temperature. The minimization of F with respect to the invariants gives the critical temperature T^*. For the phase to be biaxial the condition $\delta^3 \neq 6\Delta^2$ must be satisfied. From Fig. 4 the temperature dependences of the invariants δ and Δ are clearly found to be nonlinear, which signify the importance of the δ^3 term in F. Only five factors, c/α, d/α, e'/α, b/e, and d/e, are varied for fitting the model to the data. Figure 3 shows that S and P are reproduced extremely well by the model (except for a narrow range of temperatures at the I-N transition due to a weak first-order transition). Results for tetrapode ***B*** [Fig. 1(b)], not given here, are found to be similar to those for ***A*** [Fig. 1(a)] except for a very narrow temperature range of the N_U phase. The fitting shows that the results can be described by the mean-field model of a biaxial nematic phase where the last term is also important.

The phase diagram for the tetrapodes can be interpreted in terms of the mean-field model of Sonnet *et al.* [25], which employs a shape anisotropy λ of the biaxial dielectric susceptibility, and reduced temperature $1/\beta$ ($\beta = U_0/kT$, U_0 is the interaction energy) [25]. In the plane of $(\lambda, 1/\beta)$, a sequence of phases dependent on λ is shown in Fig. 5 where solid and broken lines represent the first- and the second-order transitions, respectively. The point where these lines meet is the tricritical point $(\lambda_t, 1/\beta)$ with $\beta_t = 7.07$. The same sequence of phases occurs until $\lambda = \lambda_c \approx 0.22$, and for $\lambda > \lambda_c$ a direct first-order transition from I-N_B is observed without an intermediate phase N_U. The experimental values of the transition temperatures for both tetrapodes are shown on the plot. We introduced interaction energies U_0 of 3.01×10^{-20} J and 3.82×10^{-20} J for tetrapodes ***A*** and ***B*** in order to obtain I-N transition temperatures in reduced units; $1/\beta_c = 0.147$ as in the model. If we use these scaling factors for the N_U-N_B transition, we obtain $1/\beta_c$ of 0.128 and 0.146 for tetrapodes ***A*** and ***B***, respectively. The corresponding values of λ can be read from the abscissa of the plot shown in Fig. 5 as their N_U-N_B transition. These are 0.198 and 0.219 for tetrapodes ***A*** and ***B***. The shape anisotropy factor λ, using its definition, is estimated from the basic dimensions of the platelet [26]. These are found to be 0.18 and 0.22, respectively; these agree reasonably with those obtained from the phase diagram. For tetrapode ***A***, the N_U-N_B transition appears to be second order and is close to the tricritical point, while for ***B*** it is first order and close to the triple point. Thus the model is able to predict the appearance of the biaxial phase, its stability, and the nature of the phase transition.

Texture and conoscopy observations in support of the above findings are given in Fig. 6. Textures for the N_B phase for the two tetrapodes, (a) sandwiched between the

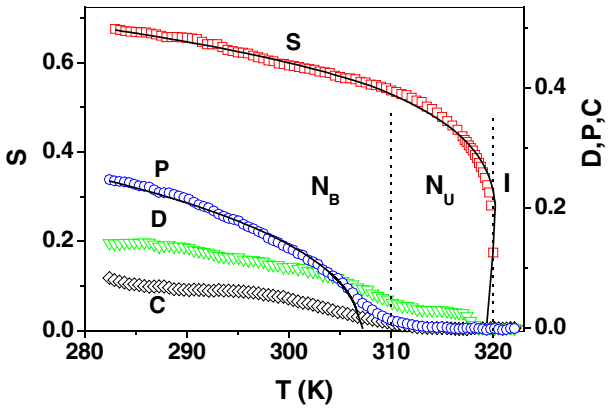

FIG. 3 (color online). Order parameters for the tetrapode ***A***: □, S; ○, P; ▽, D; ◇, C; solid line, predicted by the mean-field model [24].

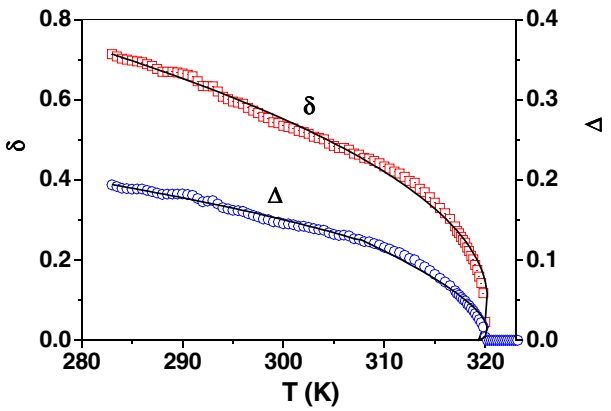

FIG. 4 (color online). Fundamental invariants of the mean-field model: □ and ○, experimentally obtained values of δ and Δ, respectively; solid lines, fits to the mean-field model [24].

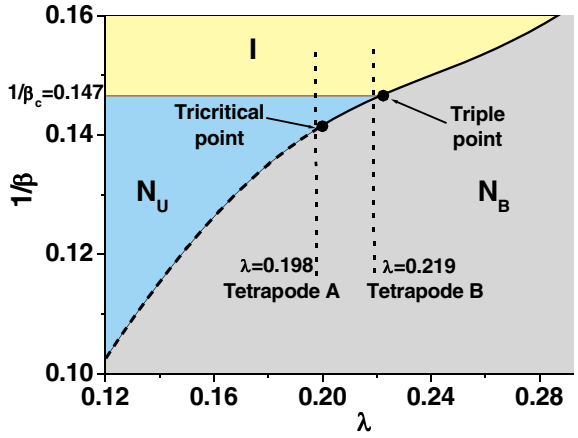

FIG. 5 (color online). Phase diagram showing the dependence of reduced temperature $1/\beta$ on the biaxiality parameter λ. Solid and broken lines exhibit phase behavior (see the text) and the vertical dotted lines give corresponding values of λ for the two tetrapodes.

two-glass plates covered by a chromolane solution (cell thickness ~ 100 μm) and (b) freestanding film of thickness ~ 25 μm, were studied. In order to achieve a complete homeotropic alignment, the cell was kept for almost 24 h at a temperature a few degrees below the I-N transition temperature. Textures for the freestanding film are given here: the Schlieren texture is comprised exclusively of two-brush disclinations [defect of strength $s = \pm 1/2$; two dark brushes meet at the disclination points; see Fig. 6(a), top]. The transition to N_U was followed with a texture change to a uniform black state [Fig. 6(c), top]. The N_U-N_B transition is confirmed by conoscopy in both cases (Fig. 6, bottom). The uniaxial cross [Fig. 6(c), bottom] clearly splits into two isogyres [Fig. 6(b), bottom]. The separation of the isogyres increases with a decrease in temperature, which consequently confirms an increase in the biaxiality [Fig. 6(a), bottom]. The molecular biaxiality in N_B seems to play an important role as observed by the intrinsic biaxiality parameters D and C found to be significantly large and increasing with decreasing temperature.

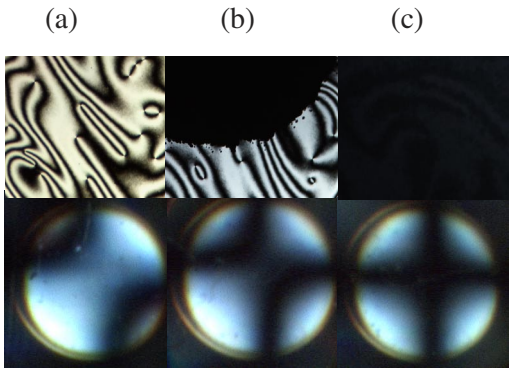

FIG. 6 (color online). Textures (top) and conoscopy (bottom) for a freestanding film of tetrapode A: (a) biaxial nematic phase; (b) phase transition between the uniaxial and biaxial nematic phases; (c) uniaxial nematic phase.

This work was supported by the EU (network project LCDD) and by SFI (02/IN.1/I031). A. K. and R. K. also acknowledge the support of the CSR, KBN 2P03B 07025. We thank C. Cruz and A. Fukuda for useful discussions and A. D. L. Chandani for help.

*Electronic address: jvij@tcd.ie

[1] M. J. Freiser, Phys. Rev. Lett. **24**, 1041 (1970).
[2] L. I. Yu and A. Saupe, Phys. Rev. Lett. **45**, 1000 (1980).
[3] G. R. Luckhurst and S. Romano, Mol. Phys. **40**, 129 (1980).
[4] J. Malthête, H. T. Nguyen, and A. M. Levelut, J. Chem. Soc. Chem. Commun. 1548 (1986).
[5] S. Chandrasekhar, B. R. Ratna, B. K. Sadashiva, and V. N. Raja, Mol. Cryst. Liq. Cryst. **165**, 123 (1988).
[6] H. F. Leube and H. Finkelmann, Makromol. Chem. **192**, 1317 (1991).
[7] J-F. Li, V. Percec, C. Rosenblatt, and O. D. Lavrentovich, Europhys. Lett. **25**, 199 (1994).
[8] A. G. Vanakaras and D. J. Photinos, Mol. Cryst. Liq. Cryst. Sci. Technol., Sect. A **299**, 65 (1997).
[9] L. Longa, J. Stelzer, and D. Dunmur, J. Chem. Phys. **109**, 1555 (1998).
[10] R. Pratiba, N.V. Madhusudana, and B. K. Sadashiva, Science **288**, 2184 (2000).
[11] C. Chiccoli, I. Feruli, O. D. Lavrentovich, P. Pasini, S.V. Shiyanovskii, and C. Zannoni, Phys. Rev. E **66**, 030701(R) (2002).
[12] G. R. Luckhurst, Thin Solid Films **393**, 40 (2001).
[13] K. Praefcke, Braz. J. Phys. **32**, 564 (2002).
[14] L. A. Madsen, T. J. Dingemans, M. Nakata, and E. T. Samulski, Phys. Rev. Lett. **92**, 145505 (2004).
[15] B. R. Acharya, A. Primak, and S. Kumar, Phys. Rev. Lett. **92**, 145506 (2004).
[16] G. R. Luckhurst, Nature (London) **430**, 413 (2004).
[17] K. Severing and K. Saalwächter, Phys. Rev. Lett. **92**, 125501 (2004).
[18] C. Tschierske, J. Mater. Chem. **11**, 2647 (2001).
[19] C. Cruz *et al.*, in *Abstracts of the 19th ILCC, Edinburgh, UK, 2002* (Royal Society of Chemistry, Cambridge, 2002). p. 314; P. Kouwer, T. Meyer and G. H. Mehl, in *Abstracts of the ECLC, Jaca, Spain, 2003* (University of Zaragoza, Zaragoza, 2003); C. Cruz *et al.* (private communication).
[20] R. Wrzalik, K. Merkel, A. Kocot, J. K. Vij and G. H. Mehl (to be published).
[21] J. P. Straley, Phys. Rev. A **10**, 1881 (1974).
[22] D. Dunmur and K. Toriyama, in *Handbook of Liquid Crystals*, edited by D. Demus *et al.* (Wiley-VCH, Weinham, 2001), Chap. VII, Vol. 1A, p. 189.
[23] K. Merkel, A. Kocot, J. K. Vij, G. H. Mehl, and T. Meyer, J. Chem. Phys. **121**, 5012 (2004).
[24] P. G. de Gennes, and J. Prost, *The Physics of Liquid Crystals* (Oxford Science, Oxford, 1993), 2nd ed.
[25] A. M. Sonnet, E. G. Virga, and G. E. Durand, Phys. Rev. E **67**, 061701 (2003).
[26] R. Berardi and C. Zannoni, J. Chem. Phys. **113**, 5971 (2000).